

**Draft Technical Memorandum**

**Title: Ultra-High-Performance Concrete (UHPC) Use in Florida Structural Applications**

**FDOT Contract Number: BDV31 977-105**

**Task 2: Acquisition and Characterization of Materials for UHPC Specimen Fabrication**

Submitted to  
The Florida Department of Transportation Research Center  
605 Suwannee Street, MS 30 Tallahassee, FL 32399

c/o Dr. Harvey DeFord, Ph.D.  
Steve Nolan, P.E.

Submitted by:

Dr. Kyle A. Riding (kyle.riding@essie.ufl.edu) (Principal Investigator)  
Dr. Christopher C. Ferraro (Co Principal Investigator)  
Dr. Trey Hamilton (Co Principal Investigator)  
Dr. Joel Harley (Co Principal Investigator)  
Megan Voss  
Raid Alrashidi  
Daniel Alabi  
Engineering School of Sustainable Infrastructure and Environment  
University of Florida  
Gainesville, Florida 32611

---

**July 2019**

**Department of Civil Engineering**

**Engineering School of Sustainable Infrastructure and Environment**

**College of Engineering**

**University of Florida**

**Gainesville, Florida 32611**

### **Disclaimer**

The opinions, findings, and conclusions expressed in this publication are those of the authors and not necessarily those of the State of Florida Department of Transportation or the U.S. Department of Transportation.

Prepared in cooperation with the State of Florida Department of Transportation and the U.S. Department of Transportation.

## Approximate Conversions to SI Units (from FHWA)

| Symbol  | When You Know               | Multiply By                 | To Find                | Symbol            |
|---|-----------------------------|-----------------------------|------------------------|-------------------|
| <b>Length</b>   |                             |                             |                        |                   |
| <b>in</b>   | inches                      | 25.4                        | millimeters            | mm                |
| <b>ft</b>   | feet                        | 0.305                       | meters                 | m                 |
| <b>yd</b>   | yards                       | 0.914                       | meters                 | m                 |
| <b>mi</b>   | miles                       | 1.61                        | kilometers             | km                |
| <b>Area</b>   |                             |                             |                        |                   |
| <b>in<sup>2</sup></b>   | square inches               | 645.2                       | square millimeters     | mm <sup>2</sup>   |
| <b>ft<sup>2</sup></b>   | square feet                 | 0.093                       | square meters          | m <sup>2</sup>    |
| <b>yd<sup>2</sup></b>   | square yard                 | 0.836                       | square meters          | m <sup>2</sup>    |
| <b>mi<sup>2</sup></b>   | square miles                | 2.59                        | square kilometers      | km <sup>2</sup>   |
| <b>Volume</b>   |                             |                             |                        |                   |
| <b>fl oz</b>  | fluid ounces                | 29.57                       | milliliters            | mL                |
| <b>gal</b>  | gallons                     | 3.785                       | liters                 | L                 |
| <b>ft<sup>3</sup></b>   | cubic feet                  | 0.028                       | cubic meters           | m <sup>3</sup>    |
| <b>yd<sup>3</sup></b>   | cubic yards                 | 0.765                       | cubic meters           | m <sup>3</sup>    |
| <b>NOTE:</b> volumes greater than 1000 L shall be shown in m <sup>3</sup> |                             |                             |                        |                   |
| <b>Mass</b>   |                             |                             |                        |                   |
| <b>oz</b>   | ounces                      | 28.35                       | grams                  | g                 |
| <b>lb</b>   | pounds                      | 0.454                       | kilograms              | kg                |
| <b>Temperature (exact degrees)</b>  |                             |                             |                        |                   |
| <b>°F</b>   | Fahrenheit                  | 5 (F-32)/9<br>or (F-32)/1.8 | Celsius                | °C                |
| <b>Illumination</b>   |                             |                             |                        |                   |
| <b>fc</b>   | foot-candles                | 10.76                       | lux                    | lx                |
| <b>fl</b>   | foot-Lamberts               | 3.426                       | candela/m <sup>2</sup> | cd/m <sup>2</sup> |
| <b>Force and Pressure or Stress</b>                                       |                             |                             |                        |                   |
| <b>lbf</b>  | pound-force                 | 4.45                        | newtons                | N                 |
| <b>lbf/in<sup>2</sup></b>   | pound-force per square inch | 6.89                        | kilopascals            | kPa               |

## I. Activities Performed During Period project start to 07/15/19

### TASK 2 – Acquisition and Characterization of Materials for UHPC Specimen Fabrication

Status: This task is complete

#### 1 Aggregate Properties

Sand was obtained for the project from Edgar Minerals. Because of the improved behavior associated with small particle sizes, a fine masonry sand was selected. No coarse aggregate was selected for this project due to its lack of use in UHPC mixes. The sand was tested according to ASTM C128 [1] to determine the specific gravity and absorption. These results are shown in Table 1. Particle size distribution was determined using ASTM C136 [2]. These results are shown in Table 2. The sand was shown to have a fineness modulus of 1.40.

Table 1 Fine aggregate relative density and absorption

|   |        |
|---|--------|
| Relative Density (Specific Gravity) (Oven Dry)              | 2.63   |
| Relative Density (Specific Gravity) (Saturated Surface Dry) | 2.64   |
| Apparent Relative Density (Specific Gravity)                | 2.66   |
| Absorption  | 0.20 % |

Table 2 Fine aggregate particle size distribution

| Sieve Size | Percent Retained | Cumulative Percent Retained |
|------------|------------------|-----------------------------|
| No.4       | 0.0              | 0.0                         |
| No. 8      | 0.1              | 0.1                         |
| No. 16     | 0.4              | 0.5                         |
| No. 30     | 3.7              | 4.2                         |
| No. 50     | 37.1             | 41.4                        |
| No. 100    | 52.7             | 94.1                        |
| No. 200    | 5.6              | 99.7                        |
| Pan        | 0.3              | 100.0                       |

#### 2 Fibers

Two different steel fibers were ordered. Steel was selected because this is the predominant material used in UHPC mixes. Polypropylene fibers are rarely used as the only fiber in a UHPC

mix due to its relatively low modulus of elasticity. The properties of the steel fibers used are presented in Table 3. Depending on results, different fiber lengths or materials may be ordered in the future for this project.

Table 3 Fiber properties

|              | <b>Bekaert Straight Fibers</b> | <b>Helix Twisted Fibers</b> |
|--------------|--------------------------------|-----------------------------|
| Diameter     | 0.0078 in. (0.2 mm)            | 0.0197 in. (0.5 mm)         |
| Length       | 0.5 in. (13 mm)                | 0.5 in. (13 mm)             |
| Coating      | brass                          | uncoated                    |
| Shape        | straight                       | twisted                     |
| Aspect Ratio | 65                             | 26                          |
| Strength     | 377.1 ksi (2600 MPa)           | 246.5 ksi (1700 MPa)        |

### 3 **Cementitious Materials**

Cement and supplementary cementitious materials were obtained for use in the project. Because of the focus on designing non-proprietary UHPCs from materials local to Florida, an ASTM C595 [3] type IL cement was selected, along with an ASTM C618 [4] Class F fly ash and an ASTM C989 [5] slag cement. An ASTM C618 metakaolin and an ASTM C1240 [6] silica fume were also procured. Additional cementitious materials may be procured in the future based on test results and new materials becoming available.

All five of the cementitious materials were analyzed using X-ray fluorescence (XRF) at the University of Florida. Specimens were prepared by Raid Alrashidi and Megan Voss, and the analyses were performed by Dr. Ann Hetherington. The standards used are shown in Table 4. The results of the XRF analyses are listed in Table 5.

Table 4 References used for XRF

| %                              | CCRL #190        |          |              | CCRL #175        |          |              | AGV-1            |          |              | Slag BFS SL-1    |          |              | Silica Stone R405 |          |              |
|--------------------------------|------------------|----------|--------------|------------------|----------|--------------|------------------|----------|--------------|------------------|----------|--------------|-------------------|----------|--------------|
|                                | Standard Average | Measured | % difference | Standard Average  | Measured | % difference |
| SiO <sub>2</sub>               | 19.60            | 19.91    | 1.60         | 18.71            | 19.08    | 1.99         | 59.88            | 60.04    | 0.27         | 35.73            | 34.63    | -3.07        | 98.03             | 98.09    | 0.06         |
| TiO <sub>2</sub>               | 0.25             | 0.25     | -0.40        | 0.33             | 0.32     | -2.42        | 1.07             | 1.05     | -1.50        |                  | 0.36     |              | 0.02              | 0.03     | 45.00        |
| Al <sub>2</sub> O <sub>3</sub> | 4.74             | 4.80     | 1.33         | 5.60             | 5.66     | 3.11         | 17.46            | 17.50    | 0.20         | 9.63             | 9.39     | -2.49        | 1.07              | 1.02     | 4.58         |
| Fe <sub>2</sub> O <sub>3</sub> | 3.03             | 3.03     | 0.07         | 2.53             | 2.48     | -1.94        | 6.88             | 6.84     | -0.63        | 1.18             | 1.03     | -12.54       | 0.05              | 0.08     | 64.00        |
| MnO                            | 0.07             | 0.09     | 22.86        | 0.10             | 0.10     | -2.00        | 0.09             | 0.14     | 56.67        |                  | 0.87     |              | 0.00              | 0.06     |              |
| MgO                            | 4.58             | 4.49     | -2.03        | 3.96             | 3.85     | -2.83        | 1.56             | 1.83     | 17.50        | 12.27            | 12.68    | 3.36         | 0.02              | 0.07     | 230.00       |
| CaO                            | 63.51            | 63.48    | 0.04         | 64.87            | 63.76    | -1.71        | 5.03             | 4.85     | -3.68        | 32.48            | 37.58    | 0.25         | 0.03              | 0.03     | -10.00       |
| NaO                            | 0.26             | 0.25     | -5.77        | 0.35             | 0.30     | -14.86       | 4.34             | 4.32     | -0.41        |                  | 0.34     |              | 0.06              | 0.10     | 63.33        |
| K <sub>2</sub> O               | 0.85             | 0.77     | -9.53        | 0.85             | 0.77     | -9.06        | 2.94             | 3.02     | 1.96         |                  | 0.50     |              | 0.71              | 0.78     | 9.86         |
| P <sub>2</sub> O <sub>5</sub>  | 0.10             | 0.11     | 13.00        | 0.24             | 0.25     | 2.92         | 0.50             | 0.51     | 1.60         |                  | 0.01     |              | 0.00              | -0.01    |              |
| SO <sub>3</sub>                | 3.32             | 3.34     | 0.51         | 3.50             | 3.08     | 0.98         | 0.11             |          |              | 3.15             | 3.03     | -3.94        | 0.00              | 0.05     |              |

Table 5 Cementitious material composition as measured by XRF

| Material        | SiO <sub>2</sub><br>wt% | TiO <sub>2</sub><br>wt% | Al <sub>2</sub> O <sub>3</sub><br>wt% | Fe <sub>2</sub> O <sub>3</sub><br>wt% | MnO<br>wt% | MgO<br>wt% | CaO<br>wt% | Na <sub>2</sub> O<br>wt% | K <sub>2</sub> O<br>wt% | P <sub>2</sub> O <sub>5</sub><br>wt% | SO <sub>3</sub><br>wt% | LOI<br>wt% |
|-----------------|-------------------------|-------------------------|---------------------------------------|---------------------------------------|------------|------------|------------|--------------------------|-------------------------|--------------------------------------|------------------------|------------|
| Cement IL       | 18.82                   | 0.22                    | 4.79                                  | 3.10                                  | 0.06       | 0.80       | 62.85      | 0.08                     | 0.25                    | 0.41                                 | 3.02                   | 5.45       |
| Slag            | 34.79                   | 0.64                    | 13.17                                 | 0.78                                  | 0.32       | 4.66       | 43.71      | 0.19                     | 0.41                    | 0.04                                 | 3.00                   | 0.02       |
| Class F Fly Ash | 57.31                   | 1.03                    | 22.59                                 | 6.76                                  | 0.06       | 2.02       | 3.37       | 0.54                     | 2.27                    | 0.24                                 | 0.49                   | 2.8        |
| Silica Fume     | 80.45                   | 0.02                    | 0.48                                  | 4.78                                  | 0.44       | 10.43      | 0.95       | 0.18                     | 0.77                    | 0.03                                 | 0.07                   | 2.93       |
| Metakaolin      | 47.41                   | 1.51                    | 41.14                                 | 0.44                                  | 0.05       | 0.00       | 0.05       | 0.20                     | 0.18                    | 0.04                                 | 0.04                   | 0.68       |

The type II cement was analyzed using X-ray diffraction (XRD). This method detects the crystalline phases of the cement, and Rietveld refinement was used to determine the percentages of each phase present in the cement. The PANalytical X'Pert powder diffraction machine at the University of Florida Nanoscale Research Facility was used. The scan was performed over a  $2\theta$  angle range of  $8^\circ$  to  $80^\circ$ . A step size of 0.008 was used with each step lasting 10 seconds. The voltage was set to 45kV, and the current was 40 mA. Soller slits of 0.04 radians were used for the X-ray tube. Divergence slits and anti-scatter slits, each at  $1^\circ$ , were used. A fixed incident beam mask was also used. The software Profex was used for the Rietveld refinement analysis. Results are presented in Table 6.

Table 6 Cement composition from X-ray diffraction

| <b>Phase</b>           | <b>Percent</b> |
|------------------------|----------------|
| Alite                  | 44.26          |
| Belite                 | 23.19          |
| Orthorhombic Aluminate | 3.47           |
| Cubic Aluminate        | 0.65           |
| Ferrite                | 11.19          |
| Bassanite              | 0.49           |
| Gypsum                 | 5.10           |
| Calcite                | 11.65          |

Thermogravimetric analysis (TGA) was used to measure the calcite content of the cement. The mass loss between approximately  $700^\circ\text{C}$  and  $800^\circ\text{C}$  was attributed to  $\text{CO}_2$  released from decomposition of calcite, and the mass loss was used to back-calculate the original mass of calcite. The calcite was determined to be 8.95% of the cement by weight.

The particle size distribution of the cementitious materials was determined using the HORIBA laser particle size analyzer (LPSA) at the State Materials Office of the Florida Department of Transportation. Each sample was run multiple times with increasing levels of ultrasonic treatment available in the laser particles size analyzer. The silica fume was sonicated with an external ultrasonic probe that provided significantly more power than the sonicator in the LPSA. This was done because laser particle size analysis done on densified silica fume often gives results showing larger particles than those actually present because the densified (intentionally agglomerated for safer handling) silica fume particles are hard agglomerates that are difficult to

disperse into the individual crystallites that make up the densified particles. Sonication helps to break up the clumps of silica particles and give a more realistic distribution [7]. The final silica fume particle size distribution was measured after the densified particles were sonicated for 7.5 minutes with the external ultrasonic probe.

The median particle size of each material is shown in Table 7. Particle size distributions are shown in

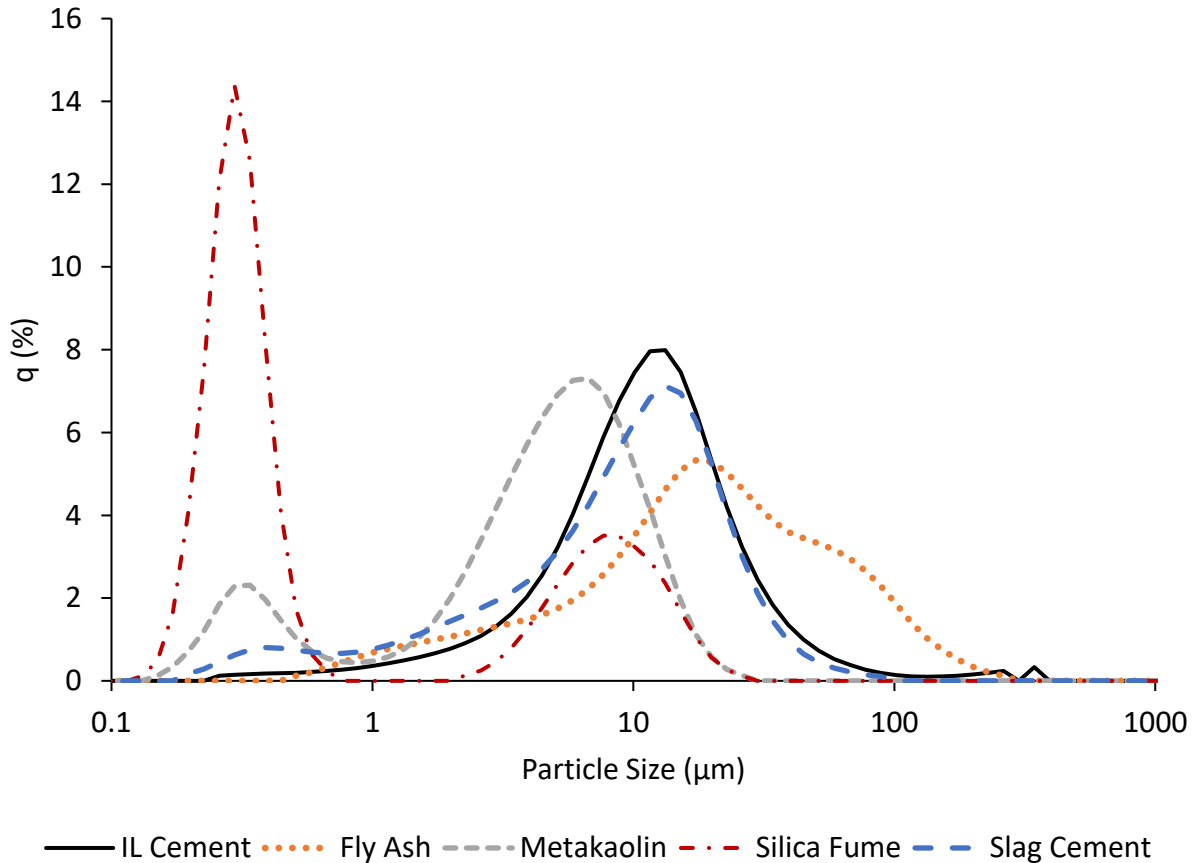


Figure 1. Cumulative particle size distribution graphs are found in Figure 2. As seen in Figure 1, both metakaolin and silica fume have bimodal particle size distributions. For silica fume, it is likely that the peak in the higher particle size range is actually because of agglomerates of smaller silica fume particles that were not separated during sonication.

Table 7 Median particle size of cementitious materials

| Material       | D <sub>50</sub> (micrometers) |
|----------------|-------------------------------|
| Type IL Cement | 10.6                          |
| Fly Ash        | 17.7                          |
| Slag           | 9.24                          |

|             |       |
|-------------|-------|
| Silica Fume | 0.329 |
| Metakaolin  | 4.56  |

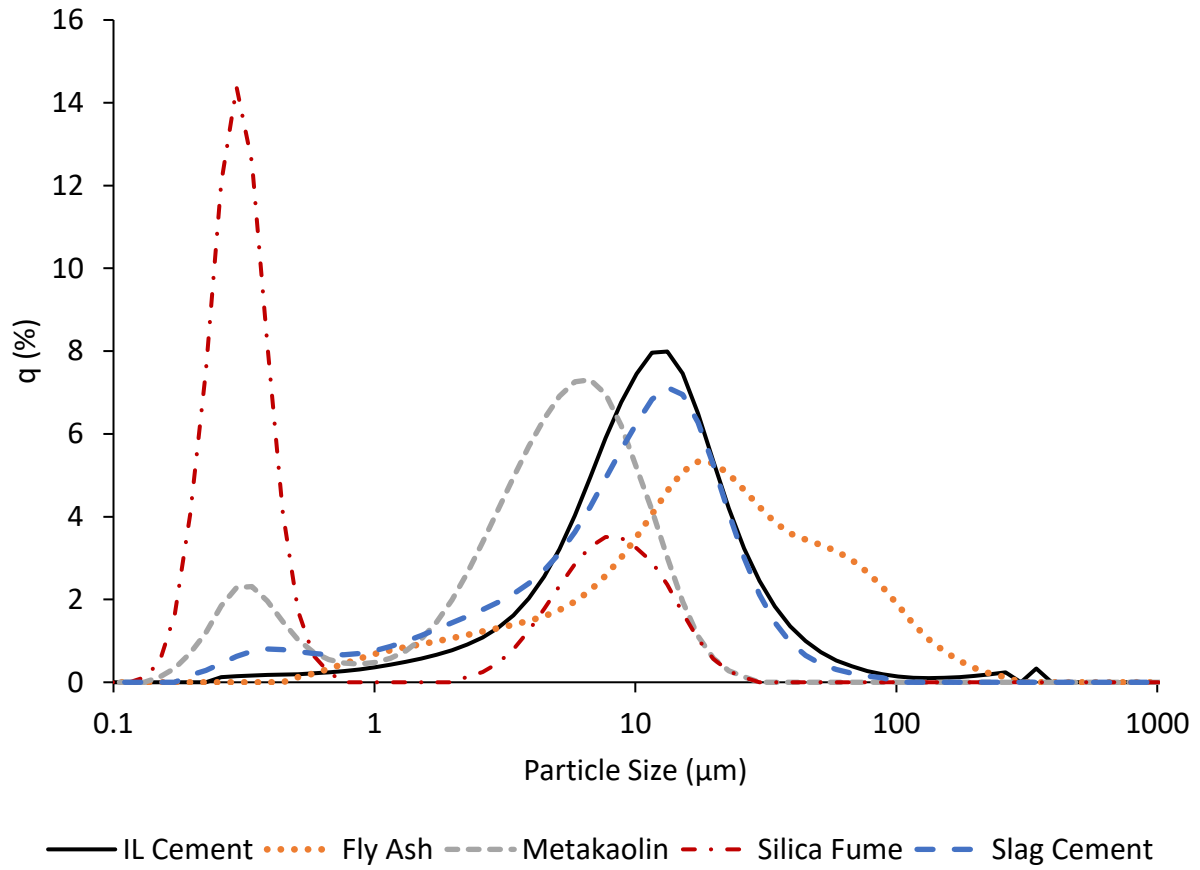


Figure 1 Particle size distribution measured by laser particle size analysis

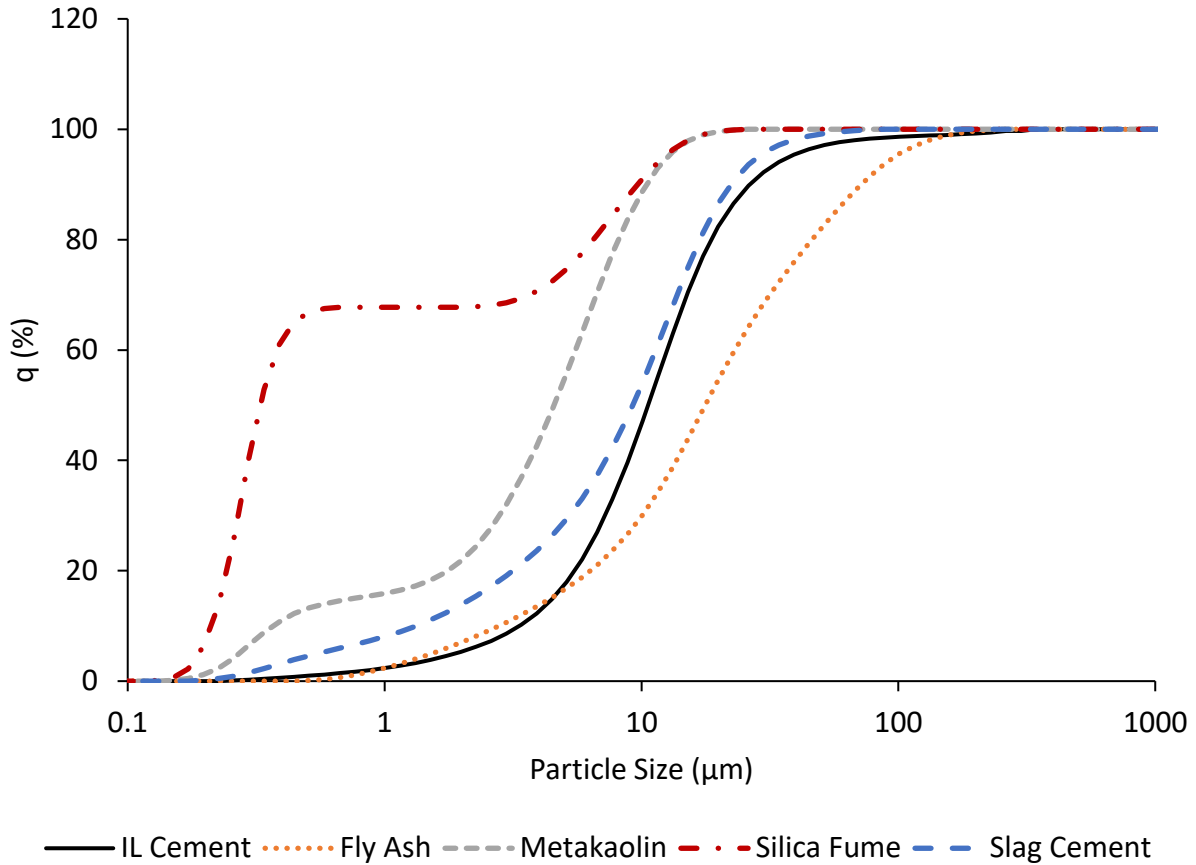


Figure 2 Cumulative particle size distribution measured by laser particle size analysis

The densities of the cementitious materials were measured using a helium pycnometer at the Nanoscale Research Facility at the University of Florida. A Quantachrome Ultrapyc 1000 gas pycnometer was used in this analysis. The material density results are presented in Table 8.

Table 8 Material specific gravities

| Material       | Average Specific Gravity |
|----------------|--------------------------|
| Type IL Cement | 3.11                     |
| Fly Ash        | 2.39                     |
| Slag           | 2.89                     |
| Silica Fume    | 2.48                     |
| Metakaolin     | 2.62                     |

4 **Planned testing**

The materials described will be used to design non-proprietary UHPC mixes. These concretes will then be tested to characterize their durability and mechanical properties. In addition to comparing mechanical and durability properties of different concrete mixes, this research will also test the mechanical and durability properties resulting from different curing regimens. Three different curing regimens will be designed: lab curing in a fog room, steam curing, and simulated field curing.

Freeze-thaw resistance will be tested for the UHPC mixtures using ASTM C666 (ASTM C666). Two samples per mixture and curing regimen will be tested in ASTM C666 procedure A. Sample resonant frequency will be measured at least every 36 cycles for 300 cycles of freeze-thaw. Samples will be tested in low-temperature calorimetry at the FDOT State Materials Office to determine the temperature at which water freezes in UHPC and the material pore size distribution.

The porosity of the concretes will be tested using multiple methods. The low volume and connectivity of micro pores in UHPC makes it difficult to use certain durability tests that are commonly adopted for normal concrete. Concrete bulk and surface resistivity will be tested and compared with some more specialized laboratory techniques, such as mercury intrusion porosimetry (MIP). In addition, other methods that could easily be implemented in industry, such as NT Build 492 rapid chloride migration test and a new water pressure absorption test, will be performed to determine their correlations.

Resistance to fresh chloride penetration will be studied by testing the UHPC with varying levels of chlorides mixed into the concrete. Long-term durability will also be tested in the field by placing samples in the University of Florida's durability site at Seahorse Key.

Mechanical properties of UHPC and very high performance concrete (VHPC) will also be tested. The mixes will be designed to have compressive strengths ranging from 10 ksi up to above 21 ksi. In addition to testing compressive strength, creep will also be measured. Creep is currently estimated using a concrete's compressive strength, but because of the high compressive strengths and widely unknown behaviors of UHPC, the relation between creep and other properties will be investigated to provide a recommendation for designers. Eighteen UHPC samples will be creep-tested using size modifications recommended in ASTM C1856 [9]. However, the load at which creep will be tested will be determined following upcoming consultations with FDOT.

Tensile properties of UHPC will be determined using the direct tension testing procedure as designed and described in phase 1 of this project. The results of the direct tension tests will be compared to the results of simpler tests to characterize the tensile strength and ductility of the mixes. The purpose of this study is to develop an easily-executed test that can be used for quality control of non-proprietary UHPC mixes. Among the tests evaluated will be a simple flexure test, with a set-up similar to ASTM C1399 [10]. In this test, the deflection and load will be measured. This could be implemented by requiring certain loads to be met or exceeded at different deflections. The double-punch test, or Barcelona method, will also be used and compared to the direct tensile test. It is important that, in addition to finding the maximum tensile strength of a mix, the strain hardening behavior, or toughness, be measured. In addition to running these tests on mixes with different compressive strengths, these methods will also be tested on mixes using different fiber percentages as well as different fiber shapes. This will ensure that the different tests are compared over a wide range of tensile strengths and with varying post-cracking behaviors.

## References

- [1] ASTM C128, "Standard Test Method for Relative Density (Specific Gravity) and Absorption of Fine Aggregate," ASTM International, 2017, 6 pp.
- [2] ASTM C136, "Test Method for Sieve Analysis of Fine and Coarse Aggregates," ASTM International, 2014, 5 pp.
- [3] ASTM C595, "Specification for Blended Hydraulic Cements," ASTM International, 2019, 8 pp.
- [4] ASTM C618, "Specification for Coal Fly Ash and Raw or Calcined Natural Pozzolan for Use in Concrete," ASTM International, 2019, 5 pp.
- [5] ASTM C989, "Specification for Slag Cement for Use in Concrete and Mortars," ASTM International, 7 pp.
- [6] ASTM C1240, "Specification for Silica Fume Used in Cementitious Mixtures," ASTM International, 2015, 7 pp.
- [7] Erich D. Rodrigues, Lourdes Soriano, Jordi Paya, Maria Victoria Borrachero, and Jose M. Monzo, "Increase of the reactivity of densified silica fume by sonication treatment," *Untrasonics Sonochemistry*, vol. 19, no. 5, 2012, pp. 1099-1107.
- [8] ASTM C666/C666M - 15, "Standard Test Method for Resistance of Concrete to Rapid Freezing and Thawing," ASTM International, 2015, 7 pp.
- [9] ASTM C1856, "Standard Practice for Fabricating and Testing Specimens of Ultra-High Performance Concrete," ASTM International, 2017, 4 pp.
- [10] ASTM C1399, "Standard Test Method for Obtaining Average Residual-Strength of Fiber-Reinforced Concrete," ASTM International, 2015, 6 pp.